

Article

Genome-Wide Identification and Characterization of the *FAR1/FHY3* Family in *Populus trichocarpa* Torr. & Gray and Expression Analysis in Light Response

Jiujun Du ¹, Lei Zhang ¹, Xiaolan Ge ¹, Xiaodong Xiang ¹, Demei Cao ¹, Haifeng Yang ^{2,*} and Jianjun Hu ^{1,*}

¹ State Key Laboratory of Tree Genetics and Breeding, Key Laboratory of Tree Breeding and Cultivation of National Forestry and Grassland Administration, Research Institute of Forestry, Chinese Academy of Forestry, Beijing 100091, China; dujiujun0517@163.com (J.D.); zhang_lei1142@163.com (L.Z.); gedalan@126.com (X.G.); xiangxd0029@126.com (X.X.); caodm_ygm@163.com (D.C.)

² East Campus, College of Forestry, Inner Mongolia Agricultural University, Hohhot 010019, China

* Correspondence: haifeng@imau.edu.cn (H.Y.); hujj@caf.ac.cn (J.H.); Tel.: +86-471-4301330 (H.Y.); +86-10-62888862 (J.H.)

Abstract: Light is an important environmental factor for plant growth, and in higher plants, phytochrome A (phyA) is the predominant far-red photoreceptor, involved in various photoresponses. The *FAR1/FHY3* transcription factor family, derived from transposases, is able to regulate plant development in response to multiple photosensitizers phytochrome. In total, 51 *PtrFRSs* were identified in the poplar genome, and were divided into 4 subfamilies. Among them, 47 *PtrFRSs* are located on 17 chromosomes. Upstream cis-acting elements of the *PtrFRS* genes were classified into three categories: growth and metabolism, stress and hormone, and the hormone and stress categories contained most of the cis-acting elements. Analysis of the regulatory networks and expression patterns showed that most *PtrFRSs* responded to changes in light intensity and were involved in the regulation of phytochromes. In this study, 51 *PtrFRSs* were identified and comprehensively bioinformatically analyzed, and preliminary functional analysis and prediction of *PtrFRSs* was carried out.

Keywords: poplar; *FAR1/FHY3*; *PtrFRSs*; gene family; light



Citation: Du, J.; Zhang, L.; Ge, X.; Xiang, X.; Cao, D.; Yang, H.; Hu, J. Genome-Wide Identification and Characterization of the *FAR1/FHY3* Family in *Populus trichocarpa* Torr. & Gray and Expression Analysis in Light Response. *Forests* **2021**, *12*, 1385. <https://doi.org/10.3390/f12101385>

Academic Editor: Dylan Fischer

Received: 22 August 2021

Accepted: 8 October 2021

Published: 11 October 2021

Publisher's Note: MDPI stays neutral with regard to jurisdictional claims in published maps and institutional affiliations.



Copyright: © 2021 by the authors. Licensee MDPI, Basel, Switzerland. This article is an open access article distributed under the terms and conditions of the Creative Commons Attribution (CC BY) license (<https://creativecommons.org/licenses/by/4.0/>).

1. Introduction

Light, as an important abiotic factor for plant growth, plays an irreplaceable role in plant growth and development, both as a source of energy for biological photosynthesis and as a provider of important environmental information to plants [1]. In higher plants, phytochromes are the major photoreceptors for red (R) and far-red (FR) light (600–750 nm). There are five phytochromes (phyA–phyE) in Arabidopsis, and phytochrome A (phyA) is the main photoreceptor in the plant that is required for the photomorphogenesis in an environment with sufficient far-red light [2], making it an indispensable phytochrome for plants [3]. phyA, the only photosensitive phytochrome that can be activated by FR, is translocated to the nucleus after being activated by light [4], which is a key step in phyA signaling [5,6]. In the nucleus, phyA acts directly as a transcriptional regulator in concert with other transcription factors (e.g., a group of bHLH transcription factors called photosensitive pigment-interacting factors (*PIFs*)) to control the expression of downstream genes [7].

FAR1 (*FAR-RED-IMPAIRED RESPONSE 1*) and its homologue *FHY3* (*FAR-RED ELONGATED HYPOCOTYL 3*) genes are a class of plant-specific transposase-derived transcription factors [8,9], which are the founding members of the *FRS* (*FAR1-RELATED SEQUENCE*) and *FRF* (*FRS-RELATED FACTOR*) families. They are conserved among land plants, and act together to directly activate the transcription of *FAR-RED ELONGATED HYPOCOTYL1* (*FHY1*) and *FHY1-LIKE* (*FHL*) to regulate phyA signaling, the products of which are essential for light-induced nuclear accumulation of phyA and subsequent light response [8].

The involvement of *FAR1/FHY3* in regulating plant responses to light is one of their well-known roles. Previous studies have demonstrated that *FAR1/FHY3* are important components of the phyA signaling pathway, and recent findings have revealed that they are also regulated by phyB, phyD, and phyE [10]. *FAR1/FHY3* regulate chlorophyll biosynthesis and seedling growth via control of *HEMB1* expression in *Arabidopsis thaliana* (L.) Heynh. [11]. They can also bind directly to *CIRCADIAN CLOCK ASSOCIATED1* (*CCA1*), a key component of the core oscillator of the circadian clock, to regulate the circadian clock of plants, which demonstrates that the photosensory-signaling pathway integrates with circadian oscillators to orchestrate clock gene expression [12].

FAR1/FHY3 are also involved in other regulatory processes in the plant, such as floral bud differentiation, carbon starvation, and branching regulation. In the regulation of floral bud differentiation, *FAR1/FHY3* directly interact with proteins of three flowering-promoting *SQUAMOSA-PROMOTER BINDING PROTEIN-LIKE* (*SPL*) transcription factors, *SPL3*, *SPL4*, and *SPL5*, and inhibit their binding to the promoters of several key flowering regulatory genes, including *FRUITFUL* (*FUL*), *LEAFY* (*LFY*), *APETALA1* (*AP1*), and *MIR172C*, thus downregulating their transcript levels and delaying flowering [13,14]. *FAR1* is even involved in the process of floral bud sex differentiation [15]. *FAR1/FHY3* are also involved in the negative feedback mediation of carbon starvation and are essential for seedlings in dark environments when disruption of both *FAR1/FHY3* leads to disruption of the chloroplast envelope and cystoid membrane [16]. In addition, disruption of *FAR1/FHY3* reduces starch accumulation and alters the starch granule structure in plants [17]. *FHY3* and *FAR1* and *SMXL6/SMXL7/SMXL8* directly interact with *SPL9* and *SPL15*, suppressing its transcriptional activation of *BRC1* [18].

Poplar is an important energy and timber species with a fast growth rate, easy asexual reproduction, relatively small genome, and easy transformation [19,20]. With the successful sequencing of the *P. trichocarpa* genome, poplar has become an ideal model for the study of woody plants [21–23]. Understanding the various developmental processes in poplar will greatly facilitate the study of woody plants [24].

Although *FAR1/FHY3* genes have been identified and characterized in several plant species [25,26], there is currently no genome-wide analysis of *P. trichocarpa*. In the present study, we sought to examine, identify, and characterize *FAR1/FHY3* genes in *P. trichocarpa* by analyzing their phylogenetic relationship, and by structuring the conserved domain architecture. Additionally, we also investigated the expression patterns of *PtrFAR1/FHY3* family genes in response to changes in light intensity to predict their function. This study provides valuable information for the analysis of the structure and function of the *PtrFAR1/FHY3* family genes in *P. trichocarpa*.

2. Methods

2.1. Plant Materials

The *P. trichocarpa* plants, used in this study, provided by laboratory of Prof. Quanzi Li of State Key Laboratory of Tree Genetics and Breeding, were preserved in the tissue culture room of the Chinese Academy of Forestry. Tissue culture seedlings were cultured in a tissue culture room at the Chinese Academy of Forestry, with the light intensity and temperature set at 2500 lx and 25 °C, respectively.

2.2. Identification, Characteristic, and Location Analysis of *PtrFRSs*

The Hidden Markov Model profiles for the *FAR1* domain (PF03101) were retrieved from the Pfam database (<http://pfam.xfam.org/> (accessed on 18 June 2020)) [27] and used to identify the *PtrFAR1/FHY3*-related sequences (*FRSs*) of poplar (*E*-Value < 0.01) with HMMER 3.0 (<http://hmmer.janelia.org/> (accessed on 18 June 2020)) [28]. SMART (<http://smart.embl.de/> (accessed on 18 June 2020)) [29], Pfam (<http://pfam.xfam.org/> (accessed on 18 June 2020)) [27], and NCBI CDD (<http://www.ncbi.nlm.nih.gov/cdd/> (accessed on 18 June 2020)) were used to confirm all the candidate *PtrFRS* genes. Online website ProtParam (<https://web.expasy.org/protparam/> (accessed on 18 June 2020)) [30],

WoLF PSORT (<https://wolfsort.hgc.jp/> (accessed on 20 August 2021)), and TBtools [31] were used to analyze the characteristic, protein subcellular localization prediction, and location on the chromosomes of *PtrFRSs*, respectively.

2.3. Sequence Alignment and Phylogenetic Construction Tree of *PtrFRSs*

Sequences of protein were extracted with Bio-Linux and were used to construct the phylogenetic tree of *PtrFRSs* by MEGA X (https://www.megasoftware.net/download_win_gui (accessed on 18 June 2020)) with the Maximum Likelihood Estimate after aligned by ClustalW.

2.4. Structural Analysis of *PtrFRSs*

The protein sequences of *PtrFRS* genes were submitted to MEME (<http://meme-suite.org/> (accessed on 18 June 2020)) [32] to search for conserved motifs of *PtrFRSs*, setting the length to 6–50 and the number to 20 and other parameters were the default value. Structural information of *PtrFRSs* was extracted and TBtools [31] was used to draw the *PtrFRS* genes structural map.

2.5. Analysis of Cis-Acting Elements in the Promoter Regions of *PtrFRSs*

The region of 1500 bp upstream of the transcriptional start point of *PtrFRSs* was extracted from the *P. trichocarpa* genome, and was used to identify cis-acting elements with the PlantCARE online website (<http://bioinformatics.psb.ugent.be/webtools/plantcare/html/> (accessed on 18 June 2020)) [33] and then cis-acting elements were analyzed and classified after that.

2.6. Prediction of the Protein–Protein Interaction Network of *PtrFRSs*

The protein sequences of *PtrFRSs* were submitted to the online database STRING (<https://string-db.org/> (accessed on 15 May 2021)) [34]. For prediction and mapping of the possible protein regulatory network, the *P. trichocarpa* genes were selected as the reference. After the BLAST step, the genes with the highest score were used to construct the network, moderately increasing the number of core genes outside the *PtrFRS* genes in the network map to allow for more accurate regulatory relationships.

2.7. RNA Isolation and Expression Analysis of *PtrFRSs* Genes of Light Response

Uniformly growing seedlings were selected for 2 shade treatments: full shade was shaded with black cloth totally (0 lx, 25 °C) (full shade, FS) while low light was placed under low light (1000 lx, 25 °C) (low light, LL) and the control was incubated under normal light conditions (2500 lx, 25 °C) (CK). The experiment was conducted in a randomized block design with 2 blocks and 3 replicates in each block (6 biological replicates). Total RNA of leaves of *P. trichocarpa* was extracted using an RNAprep Pure Plant Kit (TIANGEN, Beijing, China) according to the manufacturer's protocol, and then total RNA was reverse transcribed into cDNA using a TIANScript II RT Kit (TIANGEN, Beijing, China). qPCR, using LightCycler480 II (Roche, Basel, Switzerland), was used to analyze the expression patterns of *PtrFRSs* in response to different light intensities. We did not sequence RNA from *P. trichocarpa*.

3. Results

3.1. Identification and Chromosomal Locations of *PtrFRSs*

In total, 51 *PtrFRS* genes were identified from *P. trichocarpa*. All *PtrFRS* genes were localized on chromosomes except for *PtrFRS48* to *PtrFRS51*. For each chromosome, *PtrFRSs* was localized on all except chromosomes 18 and 19, of which, chromosomes 7 and 16 had the most *PtrFRS* genes (six) and chromosomes 1, 10, 11, 12, 13 and 15 had the least number of *PtrFRS* genes, all with only one (Figure 1).

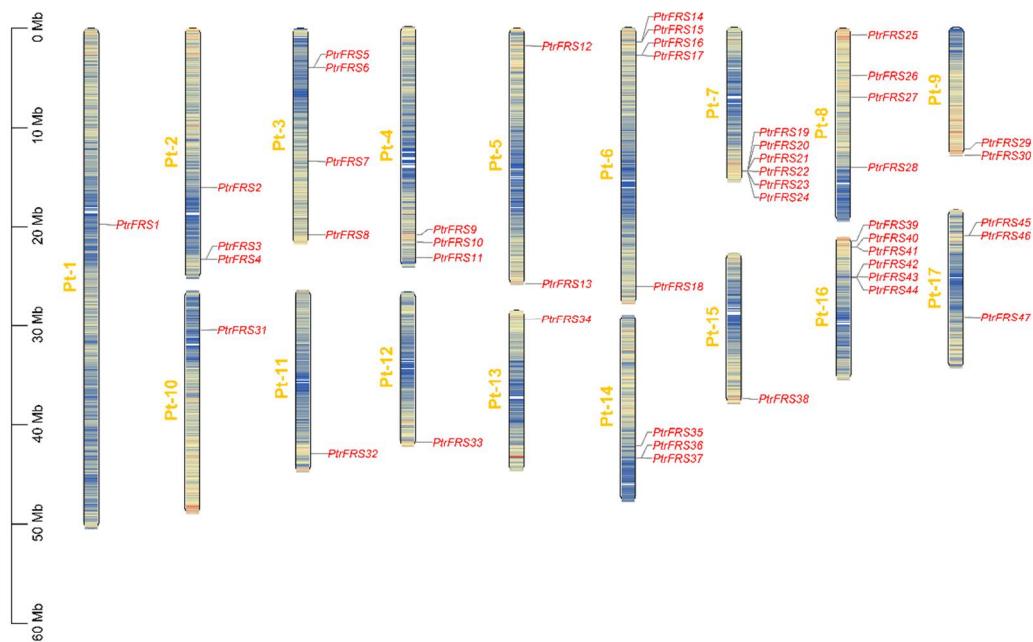


Figure 1. Chromosome localization of the *PtrFRSs*.

The *PtrFRS* genes also varied considerably among themselves, encoding amino acid numbers ranging from 107 to 902, with *PtrFRS22* and *PtrFRS29* encoding the least and most amino acid residues, respectively. Their relative molecular masses ranged from 12,473.45 to 103,330.62, with *PtrFRS22* and *PtrFRS7* being the smallest and largest, respectively. Theoretical pI ranged from 4.79 to 10.06, with *PtrFRS44* and *PtrFR22* being the smallest and largest, respectively. The grand average of hydropathicity (GRAVY) ranged from -0.939 to -0.07 , with *PtrFRS34* and *PtrFR45* being the smallest and largest, respectively. The subcellular localization of *PtrFRSs* were also predicted, with most *PtrFRS* proteins localized to the nucleus and no signal peptide predicted for all *PtrFRS* proteins (Table 1).

3.2. Phylogenetic Classification and Subfamily Division of *PtrFRSs*

A phylogenetic tree of the *PtrFRS* proteins was constructed by using the Maximum Likelihood Estimate, after aligning multiple protein sequences. The phylogenetic tree of the *PtrFRS* proteins of *P. trichocarpa* was established, and *PtrFRSs* were divided into four subfamilies (Figure 2). When classified together with the FAR1/FHY3 proteins of other species, the classification results may be more refined and precise [26], so we also constructed a phylogenetic tree of *A. thaliana* AtFRSs together with *PtrFRSs*. The results are largely consistent with the phylogenetic evolutionary tree of *PtrFRSs* (Figure S1). More sequences would make the results more accurate.

According to conservative motifs, the way in which *PtrFRSs* were grouped was further validated, with clear distinctions between each subfamily. For the motif signature of each subfamily, subfamilies I and II were significantly more complex in structure than the other two subfamilies, so it was also hypothesized that genes from these two subfamilies perform more complex functions in plants. Motifs 2, 14, 13, and 4 occurred frequently in tandem and in almost every gene (Figure 2), and the tandem sequence they comprise was identified as the FAR1 domain (Figure 2C). Following confirmation at the SMART (<http://smart.embl.de/> (accessed on 18 June 2020)), the location of the FAR1 domains was also indicated on the figure (Figure 2C).

Table 1. Information of *PtrFRS* genes.

Gene ID	Phytozome ID	Chr Location	Protein				Subcellular Localization	Signal Pep
			Length	Mw	pI	GRAVY		
<i>PtrFRS1</i>	Potri.001G201600	1	669	77,238.95	5.74	−0.426	Nucleus	NO
<i>PtrFRS2</i>	Potri.002G199300	2	759	86,585.61	5.95	−0.321	Nucleus	NO
<i>PtrFRS3</i>	Potri.002G239300	2	257	30,079.92	5.27	−0.721	Nucleus	NO
<i>PtrFRS4</i>	Potri.002G239400	2	178	20,460.26	9.61	−0.83	Nucleus	NO
<i>PtrFRS5</i>	Potri.003G031200	3	732	85,391.06	5.09	−0.566	Nucleus	NO
<i>PtrFRS6</i>	Potri.003G031400	3	658	76,223.95	8.1	−0.429	Nucleus	NO
<i>PtrFRS7</i>	Potri.003G110300	3	897	103,330.62	8.3	−0.691	Nucleus	NO
<i>PtrFRS8</i>	Potri.003G207100	3	748	86,459.71	6.81	−0.567	Nucleus	NO
<i>PtrFRS9</i>	Potri.004G196300	4	883	99,461.92	6.22	−0.495	Nucleus	NO
<i>PtrFRS10</i>	Potri.004G209000	4	789	90,574.94	6.37	−0.563	Nucleus	NO
<i>PtrFRS11</i>	Potri.004G227600	4	679	78,035.73	7.89	−0.435	Nucleus	NO
<i>PtrFRS12</i>	Potri.005G023700	5	484	54,628.34	7.81	−0.877	Nucleus	NO
<i>PtrFRS13</i>	Potri.005G257600	5	759	86,814.74	6.06	−0.495	Nucleus	NO
<i>PtrFRS14</i>	Potri.006G020600	6	842	97,070.98	6.67	−0.548	Cytoplasm	NO
<i>PtrFRS15</i>	Potri.006G020700	6	846	96,918.04	7.06	−0.674	Cytoplasm	NO
<i>PtrFRS16</i>	Potri.006G039700	6	417	46,188.23	9.29	−0.312	Nucleus	NO
<i>PtrFRS17</i>	Potri.006G039800	6	470	51,097.48	8.7	−0.267	Nucleus	NO
<i>PtrFRS18</i>	Potri.006G256300	6	670	77,830.43	6.27	−0.469	Nucleus	NO
<i>PtrFRS19</i>	Potri.007G128700	7	248	28,544.49	5.61	−0.535	Cytoplasm	NO
<i>PtrFRS20</i>	Potri.007G128800	7	253	29,360.94	5.75	−0.895	Cytoplasm	NO
<i>PtrFRS21</i>	Potri.007G128900	7	248	28,675.98	5.46	−0.923	Nucleus	NO
<i>PtrFRS22</i>	Potri.007G129000	7	107	12,473.45	10.06	−0.717	Nucleus	NO
<i>PtrFRS23</i>	Potri.007G129100	7	169	19,509.57	8.93	−0.534	Nucleus	NO
<i>PtrFRS24</i>	Potri.007G129500	7	273	31,258.18	5.72	−0.662	Nucleus	NO
<i>PtrFRS25</i>	Potri.008G011800	8	860	97,563.17	6.06	−0.432	Peroxisomes	NO
<i>PtrFRS26</i>	Potri.008G076800	8	255	28,646.2	7.09	−0.762	Nucleus	NO
<i>PtrFRS27</i>	Potri.008G108800	8	742	84,679.09	5.73	−0.326	Nucleus	NO
<i>PtrFRS28</i>	Potri.008G199300	8	830	95,699.09	8.21	−0.594	Nucleus	NO
<i>PtrFRS29</i>	Potri.009G158400	9	902	100,979.55	6.18	−0.476	Nucleus	NO
<i>PtrFRS30</i>	Potri.009G170100	9	784	89,932.74	6.99	−0.502	Nucleus	NO
<i>PtrFRS31</i>	Potri.010G029000	10	788	90,350.18	8.72	−0.514	Nucleus	NO
<i>PtrFRS32</i>	Potri.011G145800	11	807	92,308.16	6.33	−0.509	Nucleus	NO
<i>PtrFRS33</i>	Potri.012G137500	12	861	99,483.87	5.88	−0.584	Nucleus	NO
<i>PtrFRS34</i>	Potri.013G014000	13	148	16,491.42	7.73	−0.939	Nucleus	NO
<i>PtrFRS35</i>	Potri.014G167000	14	686	79,495.16	5.95	−0.413	Chloroplast	NO
<i>PtrFRS36</i>	Potri.014G176500	14	214	24,735.01	8.39	−0.866	Nucleus	NO
<i>PtrFRS37</i>	Potri.014G176600	14	207	23,296.23	6.26	−0.71	Nucleus	NO
<i>PtrFRS38</i>	Potri.015G139300	15	725	83,760.73	6.02	−0.532	Nucleus	NO
<i>PtrFRS39</i>	Potri.016G007300	16	691	80,354.36	5.87	−0.415	Nucleus	NO
<i>PtrFRS40</i>	Potri.016G018100	16	853	96,769.58	5.95	−0.43	Nucleus	NO
<i>PtrFRS41</i>	Potri.016G018300	16	843	96,537.65	7.09	−0.685	Nucleus	NO
<i>PtrFRS42</i>	Potri.016G058500	16	714	81,170.66	4.89	−0.518	Nucleus	NO
<i>PtrFRS43</i>	Potri.016G058700	16	625	72,679.85	7.21	−0.478	Nucleus	NO
<i>PtrFRS44</i>	Potri.016G059100	16	634	72,139.35	4.79	−0.538	Nucleus	NO
<i>PtrFRS45</i>	Potri.017G029100	17	250	28,553.23	6.52	−0.07	Nucleus	NO
<i>PtrFRS46</i>	Potri.017G029400	17	286	32,877.48	7.13	−0.622	Chloroplast	NO
<i>PtrFRS47</i>	Potri.017G091000	17	418	47,330.85	5.08	−0.607	Cytoplasm	NO
<i>PtrFRS48</i>	Potri.T124200	Scaffold	250	28,553.23	6.52	−0.7	Nucleus	NO
<i>PtrFRS49</i>	Potri.T124600	Scaffold	283	32,491.98	7.14	−0.657	Nucleus	NO
<i>PtrFRS50</i>	Potri.T124700	Scaffold	179	20,547.28	5.07	−0.445	Cytoplasm	NO
<i>PtrFRS51</i>	Potri.T137500	Scaffold	563	63,665.5	9.17	−0.604	Nucleus	NO

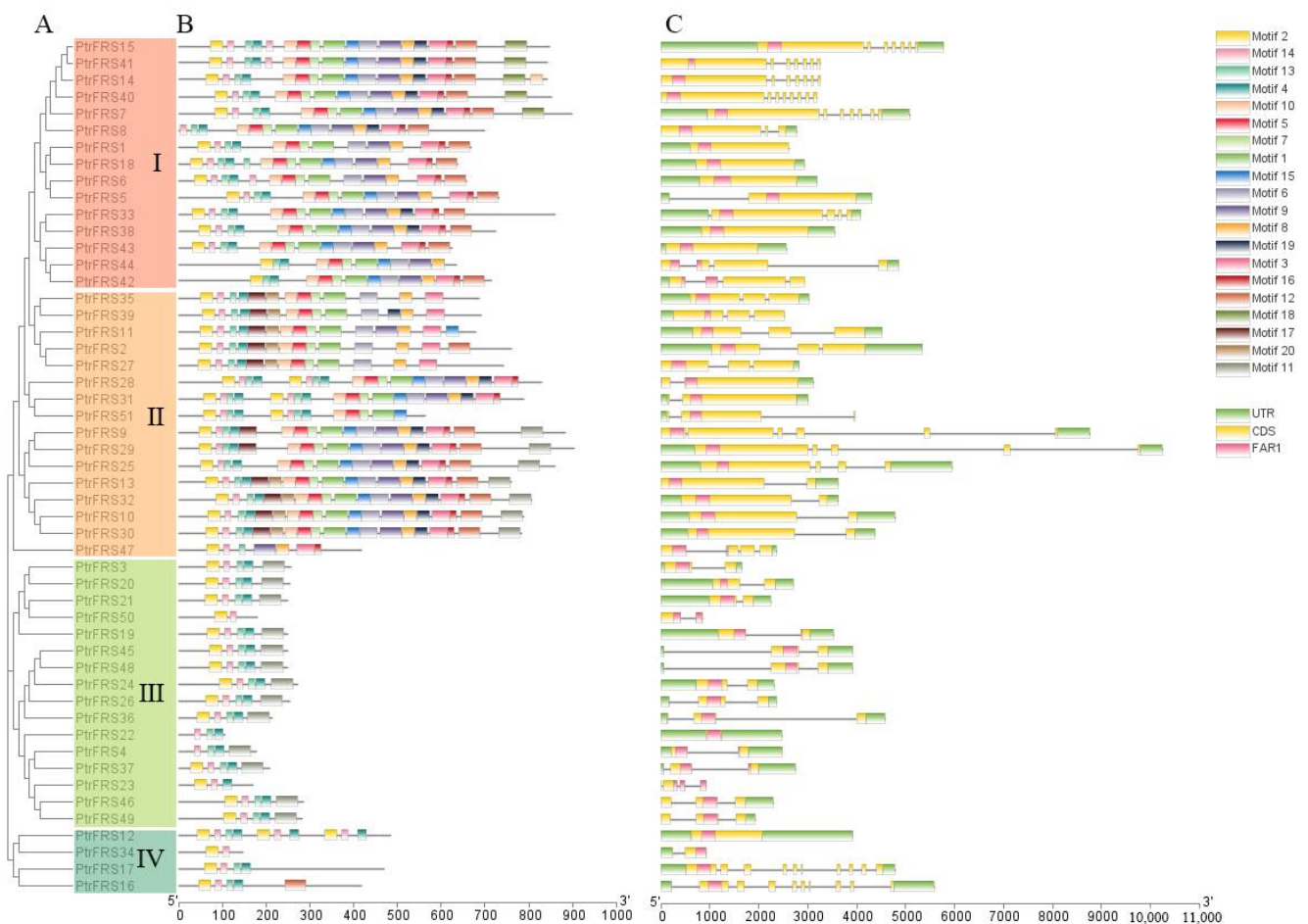


Figure 2. Phylogenetic and genetic structure analysis of *PtrFRSs*. (A) Phylogenetic tree constructed using the maximum likelihood method using 51 *PtrFRS* protein sequences and divided into four subfamilies. (B) Distribution of motifs in *PtrFRS* proteins, 20 motifs in total. (C) Structure of the *PtrFRS* genes, with the UTR in green, the FAR1 domain in pink, the exon in yellow, and the intron in the middle of the blank region.

3.3. Cis-Acting Elements of the *PtrFRSs* Promoters

The cis-acting elements in the 1500 bp region upstream of *PtrFRSs* were identified (Figure 3), analyzed, and classified into three types of hormone, stress, growth, and metabolism. The hormone type contained the most cis-acting elements, including abscisic acid, auxin, gibberellin, methyl jasmonate, salicylic acid, and ethylene. The number of cis-acting elements contained in the stress type was second only to hormone, including anaerobic induction, defense and stress, drought, low temperature, anoxic specific, dehydration, and high salt and low temperature. The growth and metabolism type contained the least, including cell cycle regulation, circadian control, cell differentiation, seed-specific regulation, endosperm expression, flavonoid biosynthetic, meristem expression, and zein metabolism regulation. Among all the cis-acting elements, there were four types of them more than 80, including abscisic acid (85), methyl jasmonate (113), ethylene (118), and anaerobic induction (98). Three of them, abscisic acid, methyl jasmonate, and ethylene, belonged to the hormone type; one belonged to stress; and none belonged to growth and metabolism. Therefore, we concluded that *PtrFRSs* play an important role in poplar hormone and stress response (Figure 4) [26]. The information regarding the cis-acting elements of each gene is also counted (Figure S2).

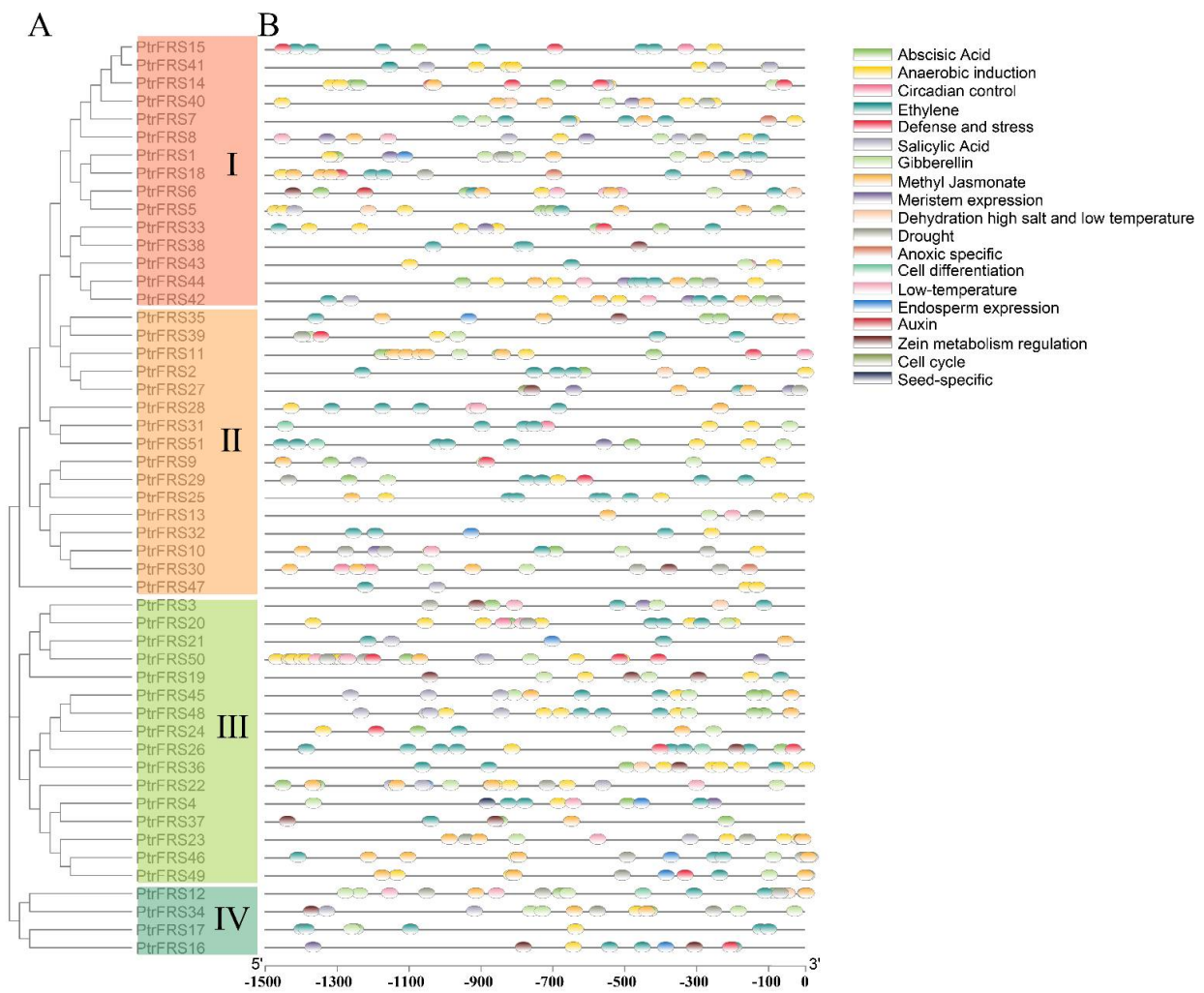


Figure 3. Analysis of the cis-acting elements of *PtrFRS*s. (A) Phylogenetic tree of *PtrFRS*s. (B) Distribution of cis-acting elements in the 1500 bp region upstream of *PtrFRS*s, with each colored oval representing a different cis-acting element.

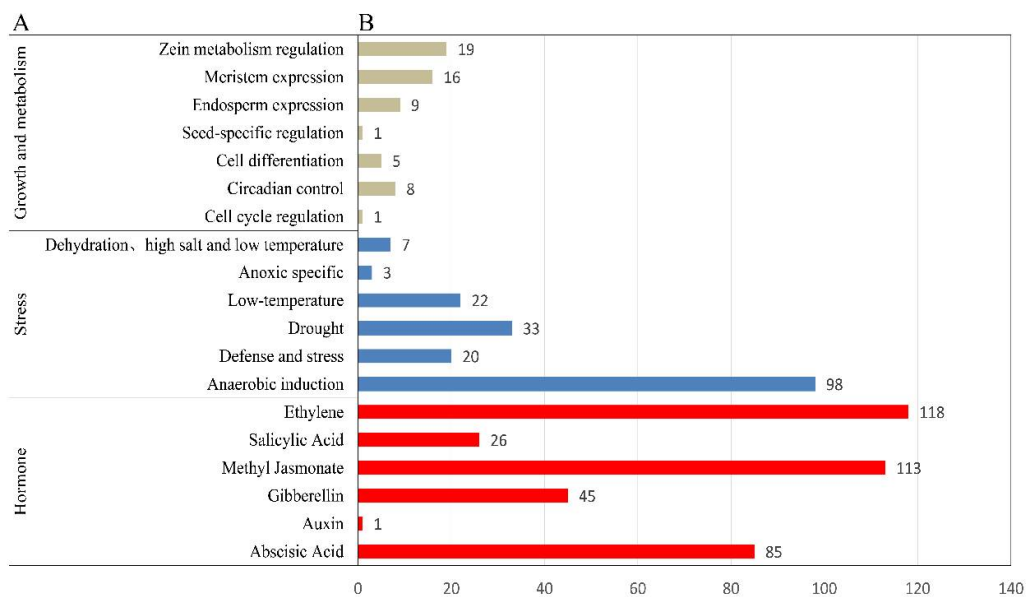


Figure 4. Statistics and classification of the cis-acting elements of *PtrFRS*s. (A) The cis-acting elements in the 1500 bp region upstream of *PtrFRS*s were divided into three groups according to their function. (B) The number of each cis-acting element of *PtrFRS*s.

3.4. Prediction of the Protein–Protein Interaction Network

The regulatory relationships of *PtrFRS* genes were predicted and elucidated. In total, 11 *PtrFRS* genes, including *PtrFRS17*, *PtrFRS18*, and *PtrFRS42*, were included in the regulatory network, and the phytochrome *phyA* acted as an upstream regulator of the *PtrFAR1/FHY3* genes, directly regulating *PtrFRS8*, *PtrFRS17*, *PtrFRS18*, *PtrFRS42* and *PtrFRS44*. Three other genes, *Pt-PIL5.1* and 2 *HY5-LIKE* genes, also interacted with several genes in the regulatory network. In addition, *PtrFRS5* interacts with two MYB proteins: MYB88 and mybMYB100 (Figure 5).

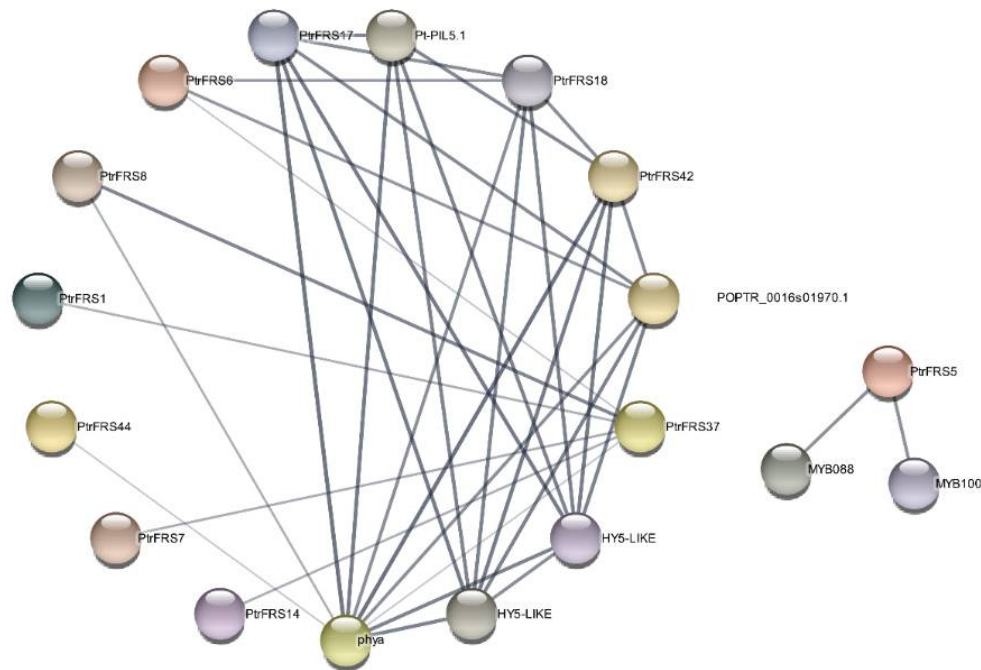


Figure 5. Predictive analysis of the PtrFREs regulatory networks.

3.5. Transcriptional Expression of *PtrFRS*s Genes during Light Reponses

The expression patterns of 51 *PtrFRS* genes under different light conditions were examined by qPCR using identical growth conditions of *P. trichocarpa* seedlings placed under different light conditions. The results showed that all *PtrFRS* genes showed changes in expression, but the expression patterns were different, mainly in two patterns: a positive and negative correlation between the expression and light intensity for the different light response patterns exhibited by *PtrFRS* genes. About half of the *PtrFRS* genes were negatively correlated with light intensity, with significant changes in expression compared to positively correlated genes. Among the genes that were negatively correlated with light intensity, *PtrFRS2*, *PtrFRS15*, *PtrFRS17*, *PtrFRS22*, *PtrFRS23*, *PtrFRS29*, *PtrFRS33*, *PtrFRS40*, and *PtrFRS42* showed greater changes in expression, while *PtrFRS40* and *PtrFRS42* showed the greatest changes in expression. Among the positive genes, the expression of *PtrFRS9* and *PtrFRS25* was significantly reduced (Figure 6). No clear distinction in expression patterns was shown between the subfamilies.



Figure 6. Expression patterns of *PtrFRSs* in response to changes in light intensity. CK normal light, LL low light, FS full shade. Average data with standard errors from three replicates is presented (* $p < 0.05$).

4. Discussion

4.1. Identification and Molecular Features of *PtrFRS* Proteins

The founding members of the *FAR1/FHY3* gene family, *FAR1* and *FHY3*, have been independently identified as two important signaling molecules in the PhyA-mediated FR-HIR response [35,36]. Although not much has been reported on this family, it has been studied in several plants, such as *Arabidopsis*. *AtFHY3*, *AtFAR1*, and 12 other *AtFRSs* have been identified [25]. In this research, HMMER 3.0 was used to identify the *PtrFRSs* and 51 *PtrFRS* genes were identified from *P. trichocarpa* (Table 1). Based on their structure, they were divided into four subfamilies, and each subfamily differed significantly from the other, with subfamilies I and II being more complex in terms of gene length and structure than III and IV (Figure 2).

The conserved protein motifs and gene structures of *PtrFRSs* were further investigated. During plant evolution, the structural features of genes are an important molecular basis for plant adaptation to environmental changes and for distinguishing them from other gene families [37]. Subfamilies I and II of the four subfamilies of *PtrFRSs* were more complex in terms of motif number, gene length, and gene structure, which also meant that they perform more complex functions in plants (Figure 2).

The *FAR1/FHY3* family is directly regulated by several phytochromes, such as phyA, phyB, phyD, and phyE [10], and is an essential transcription factor family in response to light changes in plants. In this research, we examined the response of *PtrFRS* genes to changes in light intensity using qPCR with different light intensities in *P. trichocarpa*. The vast majority of genes responded to changes in light intensity and exhibited two patterns of response: a positive response and negative response, with about half of the genes being negative and showing significant changes in expression compared to the positive-responding genes (Figure 6).

4.2. Potential Regulatory of *PtrFRSs*

We predicted the interactions between *PtrFRSs* and other key genes, and a total of 11 *PtrFRS* genes appeared in the regulatory network, in addition to phyA, *PIL5* and other key regulators of plant light response. phyA, an important factor in plant light regulation (Figure 5) [10], is in a regulatory relationship with six *PtrFRS* genes, and *PIL5* and *HY5* are also important regulators for light regulation in plants and had regulatory relationships with several *PtrFRS* genes [38,39]. *PtrFRS5* interacted with two MYB proteins, which were homologous to *AtMYB36*. *AtMYB36* is highly expressed in roots and is a transcription factor required for Casparian strip formation and is directly regulated by SCARECROW to regulate the transition from proliferation to differentiation in *Arabidopsis* roots [40,41], *PtrFRS5* may therefore be involved in the regulation of poplar root development.

The expression patterns of *PtrFRS* genes in response to light intensity were analyzed, and the results showed that the expression of most genes changed, showing both positive and negative patterns of correlation with light intensity. The expression of most of the changed *PtrFRS* genes was negatively correlated with light intensity, with more pronounced changes in expression compared to the other pattern, which is also consistent with supporting the involvement of *FAR1/FHY3* genes in plant photoresponses (Figure 6).

Analysis of the cis-acting elements in the 1500 bp region upstream of *PtrFRS* showed that cis-acting elements were divided into three categories: growth and metabolism, stress, and hormone, and that the hormone and stress categories contained most of the cis-acting elements. Thus, we can speculate that *PtrFRSs* also play an important role in plant response to hormonal stimuli and stresses [26].

5. Conclusions

In this study, we performed systematic bioinformatics analysis and identification of the *PtrFHY3/FAR1* family genes. A total of 51 *PtrFHY3/FAR1* genes (named *PtrFRS1–PtrFRS51*) were identified and their localization on the chromosome was clarified. The *PtrFRSs* were classified by constructing a phylogenetic tree and analyzing the protein and gene

structures of *PtrFRSs*. Cis-acting elements and protein-protein interaction networks were also predicted. The response of *PtrFRSs* to different light intensities was determined. These results clarified the bioinformatics of the *PtrFHY3/FAR1* family genes and demonstrated that *PtrFRSs* may play a role in hormone and stress response, growth and development, and light response, providing a theoretical basis for the study of the *FHY3/FAR1* family gene-mediated light response and hormone and stress response mechanisms in poplar and even other woody plants.

Supplementary Materials: The following are available online at <https://www.mdpi.com/article/10.3390/f12101385/s1>, Figure S1: Phylogenetic tree of *P. trichocarpa* and *A. thaliana*, Figure S2: Statistics on the distribution of cis-acting elements for *PtrFRSs*, Table S1: Primer sequences of *PtrFRSs* for qPCR analysis.

Author Contributions: J.H. and H.Y. designed experiments. J.D., L.Z. and X.G. analyzed the characteristics of sequence data. X.X. and D.C. performed qPCR experiment. J.D. wrote the manuscript. All authors have read and agreed to the published version of the manuscript.

Funding: This research was supported by the National Natural Science Foundation of China (32071797), the National Nonprofit Institute Research Grant of the Chinese Academy of Forestry (CAFYBB2017ZY008), and the National Key Program on Transgenic Research (2018ZX08020002).

Institutional Review Board Statement: Not applicable.

Informed Consent Statement: Not applicable.

Data Availability Statement: Not applicable.

Acknowledgments: We would like to thank Quanzi Li from State Key Laboratory of Tree Genetics and Breeding for providing the *P. trichocarpa* seedlings.

Conflicts of Interest: The authors declare no conflict of interest.

References

- Rausenberger, J.; Tscheuschler, A.; Nordmeier, W.; Wust, F.; Timmer, J.; Schafer, E.; Fleck, C.; Hiltbrunner, A. Photoconversion and nuclear trafficking cycles determine phytochrome A's response profile to far-red light. *Cell* **2011**, *146*, 813–825. [[CrossRef](#)] [[PubMed](#)]
- Bae, G.; Choi, G. Decoding of light signals by plant phytochromes and their interacting proteins. *Annu. Rev. Plant Biol.* **2008**, *59*, 281–311. [[CrossRef](#)]
- Botto, J.F.U.D.; Sanchez, R.A.; Whitelam, G.C.; Casal, J.J. Phytochrome A mediates the promotion of seed germination by very low fluences of light and canopy shade light in Arabidopsis. *Plant Physiol.* **1996**, *110*, 439–444. [[CrossRef](#)]
- Quail, P.H.; Boylan, M.T.; Parks, B.M.; Short, T.W.; Xu, Y.; Wagner, D. Phytochromes: Photosensory perception and signal transduction. *Science* **1995**, *268*, 675–680. [[CrossRef](#)]
- Kim, L.; Kircher, S.; Toth, R.; Adam, E.; Schafer, E.; Nagy, F. Light-induced nuclear import of phytochrome-A: GFP fusion proteins is differentially regulated in transgenic tobacco and Arabidopsis. *Plant J.* **2000**, *22*, 125–133. [[CrossRef](#)]
- Kircher, S.; Gil, P.; Kozma-Bognar, L.; Fejes, E.; Speth, V.; Husselstein-Muller, T.; Bauer, D.; Adam, E.; Schafer, E.; Nagy, F. Nucleocytoplasmic partitioning of the plant photoreceptors phytochrome A, B, C, D, and E is regulated differentially by light and exhibits a diurnal rhythm. *Plant Cell* **2002**, *14*, 1541–1555. [[CrossRef](#)]
- Kevei, E.; Schafer, E.; Nagy, F. Light-regulated nucleo-cytoplasmic partitioning of phytochromes. *J. Exp. Bot.* **2007**, *58*, 3113–3124. [[CrossRef](#)]
- Lin, R.; Ding, L.; Casola, C.; Ripoll, D.R.; Feschotte, C.; Wang, H. Transposase-Derived Transcription Factors Regulate Light Signaling in Arabidopsis. *Science* **2007**, *318*, 1302–1305. [[CrossRef](#)]
- Huan, L.; Wang, X.X.; Liu, W.; Li, L.; Gao, D. Expression Analysis of *FAR1/FHY3*-related Genes Involved in Nectarine Floral Buds during Dormancy Induction. *J. Shandong Agric. Univ. (Nat. Sci. Ed.)* **2017**, *48*, 229–235.
- Siddiqui, H.; Khan, S.; Rhodes, B.M.; Devlin, P.F. FHY3 and FAR1 Act Downstream of Light Stable Phytochromes. *Front. Plant Sci.* **2016**, *7*, 175. [[CrossRef](#)]
- Wang, W.; Tang, W.; Ma, T.; Niu, D.; Jin, J.B.; Wang, H.; Lin, R. A pair of light signaling factors FHY3 and FAR1 regulates plant immunity by modulating chlorophyll biosynthesis. *J. Integr. Plant Biol.* **2016**, *58*, 91–103. [[CrossRef](#)]
- Liu, Y.; Ma, M.; Li, G.; Yuan, L.; Xie, Y.; Wei, H.; Ma, X.; Li, Q.; Devlin, P.F.; Xu, X.; et al. Transcription Factors FHY3 and FAR1 Regulate Light-Induced *CIRCADIAN CLOCK ASSOCIATED1* Gene Expression in Arabidopsis. *Plant Cell* **2020**, *32*, 1464–1478. [[CrossRef](#)]

13. Xie, Y.; Zhou, Q.; Zhao, Y.; Li, Q.; Liu, Y.; Ma, M.; Wang, B.; Shen, R.; Zheng, Z.; Wang, H. FHY3 and FAR1 Integrate Light Signals with the miR156-SPL Module-Mediated Aging Pathway to Regulate *Arabidopsis* Flowering. *Mol. Plant* **2020**, *13*, 483–498. [[CrossRef](#)] [[PubMed](#)]
14. Wu, Q.; Bai, X.; Zhao, W.; Shi, X.; Xiang, D.; Wan, Y.; Wu, X.; Sun, Y.; Zhao, J.; Peng, L.; et al. Investigation into the underlying regulatory mechanisms shaping inflorescence architecture in *Chenopodium quinoa*. *BMC Genom.* **2019**, *20*, 658. [[CrossRef](#)] [[PubMed](#)]
15. Li, H.; Wang, L.; Mai, Y.; Han, W.; Suo, Y.; Diao, S.; Sun, P.; Fu, J. Phytohormone and integrated mRNA and miRNA transcriptome analyses and differentiation of male between hermaphroditic floral buds of andromonoecious *Diospyros kaki* Thunb. *BMC Genom.* **2021**, *22*, 203. [[CrossRef](#)] [[PubMed](#)]
16. Ma, L.; Li, G. Arabidopsis FAR-RED ELONGATED HYPOCOTYL3 negatively regulates carbon starvation responses. *Plant Cell Environ.* **2021**, *44*, 1816–1829. [[CrossRef](#)] [[PubMed](#)]
17. Ma, L.; Xue, N.; Fu, X.; Zhang, H.; Li, G. Arabidopsis thaliana FAR-RED ELONGATED HYPOCOTYLS3 (FHY3) and FAR-RED-IMPAIRED RESPONSE1 (FAR1) modulate starch synthesis in response to light and sugar. *New Phytol.* **2017**, *213*, 1682–1696. [[CrossRef](#)]
18. Xie, Y.; Liu, Y.; Ma, M.; Zhou, Q.; Zhao, Y.; Zhao, B.; Wang, B.; Wei, H.; Wang, H. Arabidopsis FHY3 and FAR1 integrate light and strigolactone signaling to regulate branching. *Nat. Commun.* **2020**, *11*, 1955. [[CrossRef](#)] [[PubMed](#)]
19. Bryant, N.D.; Pu, Y.; Tschaplinski, T.J.; Tuskan, G.A.; Muchero, W.; Kalluri, U.C.; Yoo, C.G.; Ragauskas, A.J. Transgenic Poplar Designed for Biofuels. *Trends Plant Sci.* **2020**, *25*, 881–896. [[CrossRef](#)]
20. Kucharska, K.; Łukajtis, R.; Słupek, E.; Cieśliński, H.; Rybarczyk, P.; Kamiński, M. Hydrogen Production from Energy Poplar Preceded by MEA Pre-Treatment and Enzymatic Hydrolysis. *Molecules* **2018**, *23*, 3029. [[CrossRef](#)]
21. Taylor, G. Populus: Arabidopsis for forestry. Do we need a model tree? *Ann. Bot.* **2002**, *90*, 681–689. [[CrossRef](#)] [[PubMed](#)]
22. Tuskan, G.A.; DiFazio, S.; Jansson, S.; Bohlmann, J.; Grigoriev, I.; Hellsten, U.; Putnam, N.; Ralph, S.; Rombauts, S.; Salamov, A.; et al. The Genome of Black Cottonwood, *Populus trichocarpa* (Torr. & Gray). *Science* **2006**, *313*, 1596–1604. [[PubMed](#)]
23. Wullschleger, S.D.; Tuskan, G.A.; DiFazio, S.P. Genomics and the tree physiologist. *Tree Physiol.* **2002**, *22*, 1273–1276. [[CrossRef](#)] [[PubMed](#)]
24. Liu, Q.; Ding, C.; Chu, Y.; Chen, J.; Zhang, W.; Zhang, B.; Huang, Q.; Su, X. PoplarGene: Poplar gene network and resource for mining functional information for genes from woody plants. *Sci. Rep.* **2016**, *6*, 31356. [[CrossRef](#)]
25. Lin, R.; Wang, H. Arabidopsis FHY3/FAR1 gene family and distinct roles of its members in light control of Arabidopsis development. *Plant Physiol.* **2004**, *136*, 4010–4022. [[CrossRef](#)]
26. Liu, Z.; An, C.; Zhao, Y.; Xiao, Y.; Bao, L.; Gong, C.; Gao, Y. Genome-Wide Identification and Characterization of the CsFHY3/FAR1 Gene Family and Expression Analysis under Biotic and Abiotic Stresses in Tea Plants (*Camellia sinensis*). *Plants* **2021**, *10*, 570. [[CrossRef](#)]
27. El-Gebali, S.; Mistry, J.; Bateman, A.; Eddy, S.R.; Luciani, A.; Potter, S.C.; Qureshi, M.; Richardson, L.J.; Salazar, G.A.; Smart, A.; et al. The Pfam protein families database in 2019. *Nucleic Acids Res.* **2019**, *47*, D427–D432. [[CrossRef](#)]
28. Johnson, L.S.; Eddy, S.R.; Portugaly, E. Hidden Markov model speed heuristic and iterative HMM search procedure. *BMC Bioinform.* **2010**, *11*, 431. [[CrossRef](#)]
29. Letunic, I.; Khedkar, S.; Bork, P. SMART: Recent updates, new developments and status in 2020. *Nucleic Acids Res.* **2021**, *49*, D458–D460. [[CrossRef](#)]
30. Wilkins, M.R.; Gasteiger, E.; Bairoch, A.; Sanchez, J.C.; Williams, K.L.; Appel, R.D.; Hochstrasser, D.F. Protein identification and analysis tools in the ExpASY server. *Methods Mol. Biol.* **1999**, *112*, 531–552.
31. Chen, C.J.; Chen, H.; Zhang, Y.; Thomas, H.R.; Frank, M.H.; He, Y.H.; Xia, R. TBtools: An integrative toolkit developed for interactive analyses of big biological data. *Mol. Plant* **2020**, *13*, 1194–1202. [[CrossRef](#)]
32. Bailey, T.L.; Boden, M.; Buske, F.A.; Frith, M.; Grant, C.E.; Clementi, L.; Ren, J.; Li, W.W.; Noble, W.S. MEME SUITE: Tools for motif discovery and searching. *Nucleic Acids Res.* **2009**, *37*, W202–W208. [[CrossRef](#)]
33. Lescot, M.; Dehais, P.; Thijs, G.; Marchal, K.; Moreau, Y.; Van de Peer, Y.; Rouze, P.; Rombauts, S. PlantCARE, a database of plant cis-acting regulatory elements and a portal to tools for in silico analysis of promoter sequences. *Nucleic Acids Res.* **2002**, *30*, 325–327. [[CrossRef](#)]
34. Szklarczyk, D.; Gable, A.L.; Lyon, D.; Junge, A.; Wyder, S.; Huerta-Cepas, J.; Simonovic, M.; Doncheva, N.T.; Morris, J.H.; Bork, P.; et al. STRING v11: Protein-protein association networks with increased coverage, supporting functional discovery in genome-wide experimental datasets. *Nucleic Acids Res.* **2019**, *47*, D607–D613. [[CrossRef](#)]
35. Hudson, M.; Ringli, C.; Boylan, M.T.; Quail, P.H. The FAR1 locus encodes a novel nuclear protein specific to phytochrome A signaling. *Genes Dev.* **1999**, *13*, 2017–2027. [[CrossRef](#)]
36. Wang, H.; Deng, X.W. Arabidopsis FHY3 defines a key phytochrome A signaling component directly interacting with its homologous partner FAR1. *EMBO J.* **2002**, *21*, 1339–1349. [[CrossRef](#)] [[PubMed](#)]
37. Jeffares, D.C.; Penkett, C.J.; Bahler, J. Rapidly regulated genes are intron poor. *Trends Genet.* **2008**, *24*, 375–378. [[CrossRef](#)]
38. Gangappa, S.N.; Botto, J.F. The Multifaceted Roles of HY5 in Plant Growth and Development. *Mol. Plant* **2016**, *9*, 1353–1365. [[CrossRef](#)]
39. Wu, M.; Liu, D.; Abdul, W.; Upreti, S.; Liu, Y.; Song, G.; Wu, J.; Liu, B.; Gan, Y. PIL5 represses floral transition in Arabidopsis under long day conditions. *Biochem. Biophys. Res. Commun.* **2018**, *499*, 513–518. [[CrossRef](#)] [[PubMed](#)]

-
40. Kamiya, T.; Borghi, M.; Wang, P.; Danku, J.M.C.; Kalmbach, L.; Hosmani, P.S.; Naseer, S.; Fujiwara, T.; Geldner, N.; Salt, D.E. The MYB36 transcription factor orchestrates Casparian strip formation. *Proc. Natl. Acad. Sci. USA* **2015**, *112*, 10533–10538. [[CrossRef](#)] [[PubMed](#)]
 41. Liberman, L.M.; Sparks, E.E.; Moreno-Risueno, M.A.; Petricka, J.J.; Benfey, P.N. MYB36 regulates the transition from proliferation to differentiation in the *Arabidopsis* root. *Proc. Natl. Acad. Sci. USA* **2015**, *112*, 12099–12104. [[CrossRef](#)] [[PubMed](#)]